Halide Ion Complexes of Decaborane ($B_{10}H_{14}$) and Their Derivatives: Noncovalent Charge Transfer Effect on Second-Order Nonlinear Optical Properties

ARTICLE *in* THE JOURNAL OF PHYSICAL CHEMISTRY A · DECEMBER 2011

Impact Factor: 2.69 · DOI: 10.1021/jp209385b · Source: PubMed

THE JOURNAL OF PHYSICAL CHEMISTRY A

Article

pubs.acs.org/JPCA

Halide Ion Complexes of Decaborane ($B_{10}H_{14}$) and Their Derivatives: Noncovalent Charge Transfer Effect on Second-Order Nonlinear Optical Properties

Shabbir Muhammad, Takuya Minami, Hitoshi Fukui, Kyohei Yoneda, Ryohei Kishi, Yasuteru Shigeta, and Masayoshi Nakano*

Department of Materials Engineering Science, Graduate School of Engineering Science, Osaka University, Toyonaka, Osaka 560-8531, Japan

Supporting Information

ABSTRACT: Quantum molecular engineering has been performed to determine the second-order nonlinear optical (NLO) properties in different halo complexes of decaborane ($B_{10}H_{14}$) and their derivatives using the density functional theory (DFT) method. These decaborane halo complexes of $X^-@B_{10}H_{14}$ (X = F, Cl, Br, and I) are found to possess noncovalent charge transfer interactions. The static polarizability (α_0) and first hyperpolarizability (β_0) among these complexes increase by moving down the group from F to I, partly due to the increase in size of their anionic radii and the decrease in their electron affinities. A two-level approximation has been employed to investigate the origin of β_0 values in these halo complexes, which show very consistent results with those by the finite-field method. Furthermore, in the same line, two experimentally existing complexes, $I^-@B_{10}H_{14}$ and $I^-@2,4\text{-}I_2B_{10}H_{12}$, are found to have considerably large β_0 values of 2859 and 3092 a.u., respectively, which are about three times larger than a prototypical second-order NLO molecule of *p*-nitroaniline, as reported by Soscun et al. [*Int. J. Quantum Chem.* **2006**, *106*, 1130−1137]. Besides this, the special effects of solvent, counterion, and bottom substitutions have also been investigated. Interestingly, 2,4-alkali metal-substituted decaborane iodide complexes show remarkably large second-order NLO response with β_0 amplitude as large as 62436 a.u. for $I^-@2,4\text{-}K_2B_{10}H_{12}$ complex, which are explained in terms of their transition energies, frontier molecular orbitals and electron density difference plots. Thus, the present investigation provides several new comparative insights into the second-order NLO properties of halo complexes of decaborane, which possess not only large first hyperpolarizabilities, but also high tunability to get a robustly large second-order NLO response by alkali metal substitution effects.

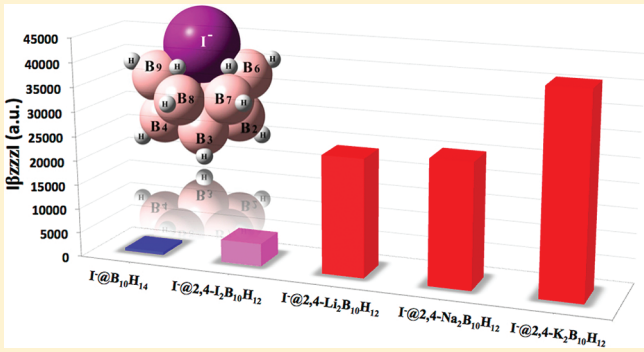

1. INTRODUCTION

The study of the second-order nonlinear optical (NLO) compounds has been of particular interest since the 1960s, when Franken et al.[1] presented the first report dealing with the production of second harmonic generation (SHG). There have been extensive research efforts to synthesize more efficient second-order NLO materials. Traditionally, second-order NLO-active molecules were discovered by numerous research efforts with only rudimentary design rules to guide such synthetic explorations. The modern synthetic chemistry of contemporary chromophores in association with reliable computational techniques has resulted in many tedious syntheses that were previously being uncertain.[2] Over the past decade, chemically oriented computational quantum procedures have been in the forefront of struggle to change the science of chromophores design. Not surprisingly, many kinds of second-order NLO materials have been proposed so far based on computationally guided synthetic strategies, most of them utilize the introduction of donor−acceptor substituents to enhance the second-order NLO properties through the induced asymmetric charge distribution.[3] Along similar lines, Coe et al.[4] have reported several combined experimental and computational studies of organometallic and inorganic second-order NLO compounds. Similarly, studies by Champagne et al.[5] to exploit second-order NLO materials can also be seen as a mile stone during the past decade. It has also been predicted that the electron correlation effects on the bond nature control the NLO properties: zwitter-ionic states in twisted π-electron NLO chromophores[6−8] cause a great enhancement of second-order NLO properties, and the diradical character is also a key factor of enhancing or tuning second-order NLO properties in open-shell asymmetric molecules, for example, diphenalenyl

Received: September 28, 2011
Revised: December 18, 2011
Published: December 30, 2011

diradicaloids.[9] Some very recent examples include second-order NLO polymeric borate clusters,[10] cationic bipyridyl iridium(III) complexes[11] and so forth.[2]

Among the huge pile of previously reviewed NLO materials,[12] some lithium and boron based second-order NLO materials including LiB_3O_5 (LBO),[13] BaB_2O_4 (BBO),[14] $BaZnBO_3F$,[15] borates,[16] and boronates[17] have been successfully commercialized. Such totally inorganic compounds have higher thermal stabilities along with good transparency trade-off values relative to the organic molecules, and hence, they are the natural candidates for the second-order NLO materials. Up to now, the inorganic molecules are the most widely used second-order NLO materials, but the relevant small photoelectric coefficients of such inorganic second-order NLO compounds are the stumbling blocks in their optimal exploitation. In our previous work, we have described a new strategy to design a lithium decaborane complex, in which the valence electron of the doped Li atom pulled into the cavity of the electron-deficient $B_{10}H_{14}$ complexant forming the excess electron.[18] In spite of the fact that these excess electron complexes showed significantly large NLO response, but the presence of acidic hydrogen atoms at open-end of $B_{10}H_{14}$ basket is a bottleneck in the syntheses of such lithiated borane complexes and their derivatives.[19−21] For our further investigation, herein we have adopted a more practical approach by selecting already synthesized $I^-@B_{10}H_{14}$ and $I^-@2,4\text{-}I_2B_{10}H_{12}$ complexes.[22] In these complexes, a single crystal X-ray analysis shows that the unique iodide ion resides on top of four bridging hydrogen atoms at the opening end of $B_{10}H_{14}$ basket. It is therefore expected that $I^-@B_{10}H_{14}$ complex might have significantly large β_0 values among all halide ion complexes due to the larger size of iodine ion. On the basis of the computational study, it could be further modified to get more polarization from the bottom substitutions in $I^-@B_{10}H_{14}$ complex that can ultimately lead to a robustly large second-order NLO response better than previously designed $Li@B_{10}H_{14}$. The present study aims to theoretically design a new realistic model second-order NLO molecule with the downward-pulling electronic effects of the $B_{10}H_{14}$ complexant. This report will not only explore the second-order NLO response of experimentally existing $I^-@B_{10}H_{14}$ and $I^-@2,4\text{-}I_2B_{10}H_{12}$ complexes, but also provide a guideline for tuning their second-order NLO responses with halo and alkali atoms substitutions at the bottom positions of these complexes.

2. COMPUTATIONAL DETAILS

The optimized geometric structures of $B_{10}H_{14}$ and $I^-@B_{10}H_{14}$ and its halo/alkali derivatives with all real frequencies were obtained using the B3LYP method[23] and the 6-31G(d) basis set for all other atoms except iodine. For iodine atoms a "double-ζ" quality basis set LANL2DZdp with effective core potential (ECP) have been used in the present investigation.[24] The ECP on iodine atom/ion replaced the inner core electrons, leaving the outer core $[(5s)^2\ (5p)^5]$ electrons as valence electrons of iodine. A detail discussion about the difference of β values by a systematic extension of basis sets on all atoms of parent system ($I^-@2,4\text{-}I_2B_{10}H_{12}$) has been given in Table S1 of Supporting Information. There are some slight oscillations among different components of β value by adding further polarization and diffuse functions, but the overall trend remains almost similar (90% on average) to the above basis set. Moreover, for the reliability of our computational method, the molecular structure has been checked by comparing the geometrical parameters with a highly correlated, coupled cluster method having single and double excitations (CCSD)[25] and experimental values.[22] We have also examined the performance of other hybrid DFT, that is, PBE0 and B3P86, and ab initio molecular orbital (MO) electron-correlation methods, that is, second-order Møller−Plesset perturbation (MP2) and CCSD for $I^-@2,4\text{-}I_2{-}B_{10}H_{12}$ complex to investigate the calculation method dependence of the polarizability and first hyperpolarizability values. The $|\beta_{zzz}|$ values with highly correlated methods are close to those with B3LYP functional calculated on the CCSD optimized geometry of $I^-@2,4\text{-}I_2{-}B_{10}H_{12}$ complex. The difference is only 2 and 6% for the CCSD and MP2 methods, respectively (see Table S2 in Supporting Information). This shows the reliability of the B3LYP functional to evaluate α and β values in present investigation. Using the ground state optimized geometries, the time-dependent (TD)-DFT[26] approach using the B3LYP functional is also applied to the investigation of the excited-state electronic properties. Besides this, solvent and counterion effects have been also checked for the calculation of different eleco-optical properties. For solvent effects, a polarized continuum method (SCRF-PCM)[27] has been used taking tetrahydrofuran as a solvent with ε value of 7.425 and Na ion as a counter positive ion according to the previous experimental study.[22] For the calculation of the second-order NLO properties, the most widely employed finite-field (FF) method is used with "Polar = Enonly" keyword in the Gaussian 09 program package.[28] When a molecule is subjected to the static electric field (F), the energy (E) of the molecule is expressed by eq 1

$$E = E^{(0)} - \mu_i F_i - \frac{1}{2}\alpha_{ij}F_iF_j - \frac{1}{6}\beta_{ijk}F_iF_jF_k - \ldots \quad (1)$$

where $E^{(0)}$ is the energy of a molecule in the absence of an electronic field, μ_i is the ith component of the dipole moment vector, α_{ij} is the linear polarizability tensor, and β_{ijk} is the first hyperpolarizability tensor, respectively, where i, j, and k label indicate the x, y, and z components. For a molecule, the dipole moment amplitude (μ_0) and average polarizability α_0 are defined as follows:

$$\mu_0 = (\mu_x^2 + \mu_y^2 + \mu_z^2)^{1/2} \quad (2)$$

For the average polarizability, we have

$$\alpha_0 = \frac{1}{3}(\alpha_{xx} + \alpha_{yy} + \alpha_{zz}) \quad (3)$$

The amplitude of first hyperpolarizability is defined as

$$\beta_0 = (\beta_x + \beta_y + \beta_z)^{1/2} \quad (4)$$

where

$$\beta_i = \frac{3}{5}\sum_j \beta_{ijj} \quad (j = x, y, z) \quad (5)$$

All calculations were performed using Gaussian 09 software package[28] with default settings, that is, energy convergence criteria 10^{-N}, where $N = 8$, field strength is 0.001 a.u., and so on.

3. RESULTS AND DISCUSSION

3.1. Geometrical Structures. We have first optimized the geometry of $I^-@2,4\text{-}I_2{-}B_{10}H_{12}$ complex that has been reported

in an experimental study[22] with its crystallographic characterization, as shown in Figure 1. Similar to the experimental

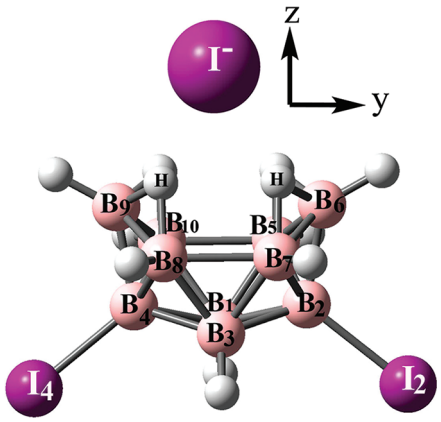

Figure 1. Label diagram of $I^-@2,4\text{-}I_2B_{10}H_{12}$ complex according to ref 22.

structure, a conformation of $B_{10}H_{14}$ with an iodine ion in the center of C_{2v} symmetry has been optimized by the B3LYP method. The calculated geometric parameters have been given in Table 1. It can be seen that the B3LYP method provides a reasonable agreement with experimental values. In Table 1, we also include the geometrical parameters calculated with a strongly correlated method, that is, CCSD (see the values in parentheses). The results obtained from the CCSD calculations are not only in agreement with experimental values, but also show the reliability of the B3LYP method for reproducing the molecular geometries examined in the present investigation.

In the present study, we have categorized the chemical models into five sets depending on the type of complexing ions (set A), substitutions at decaborane (sets B and C), with solvent (set BS), and counterion effects (set BNa). Set A includes the complexes of halide ions with decaborane. In sets B and C, bottom positions of $I^-@B_{10}H_{14}$ complex have been substituted with iodine atoms (1,3 and 2,4) and alkali metals (only 2,4), respectively, while fluoride substitution has been also made for 2,4 positions in set B. The motivation about the choice of these positions lies in the achievement of a downward pulling effect (which is expected to further enhance β) with practically realistic sites for substitutions similar to previous experimentally reported compounds of $I^-@2,4\text{-}I_2\text{-}B_{10}H_{12}$, $2,4\text{-}I_2\text{-}B_{10}H_{12}$, $2,4\text{-}D_2\text{-}B_{10}H_{12}$, and $1,3\text{-}D_2\text{-}B_{10}H_{12}$.[29] Because the geometries of systems of set B have been changed slightly after reoptimization with solvent and counterions, these systems were placed in new sets BS and BNa, with solvent and counterion effects, respectively.

A comparison of terminal bond lengths between $B_{6/9}$ and iodine ions of $I^-@B_{10}H_{14}$ complex and its derivatives shows that it ranges from 3.624 to 3.946 Å with the lowest value in $I^-@2,4\text{-}I_2{-}B_{10}H_{12}$ complex. These distances are shorter than the sum of the van der Waals radii of iodine and boron atoms, that is, 3.980 Å.[30] This represents that in our all designed derivatives the orbital interaction is effective and then is expected to significantly affect the electro-optical properties.

3.2. Electro-Optical Properties. The electronic properties including polarizablities (α_0) and first hyperpolarizabilities (β_0) of different derivatives of halo-decaborane complexes have been given in different sets of Table 2. For all the systems, dominant contributions to β_0 are found to come from β_{zzz} values. These results can be interpreted in several ways. In set A, fluoride ion shows the shortest distance from $B_{6/9}$ atoms and this complex has the lowest β_0 value of 367 a.u., which gradually increases in complexes (from system $\mathbf{A_1}$ to $\mathbf{A_4}$) of other halide ions and have the largest value of 2859 a.u. for $I^-@B_{10}H_{14}$ complex. The lighter halide anions of F, Cl, and Br are considerably smaller in size with more affinity for extra electron than that of I. Due to the increase of anionic radii of halide ions and to the decrease in the electron affinity in $X^-@B_{10}H_{14}$ (X = F, Cl, Br, and I) complexes, the α_0 and β_0 values increase as moving down the group and show maximum values in $I^-@B_{10}H_{14}$ complex. This has been explained in Figure 2 by drawing the parameters that govern the β_0 value. According to the two-level approximation (as explained in the next section), these parameters include the values of the transition energy (ΔE), change of dipole moment between the ground and crucial excited state ($\Delta\mu_z$), and transition moment (μ_z^0) along the z-axis. From Figure 2 it can be seen that the $I^-@B_{10}H_{14}$ complex ($\mathbf{A_4}$) has higher $|\Delta\mu_z|$ and $|\mu_z^0|$ along with lower ΔE values that jointly lead to larger amplitude of β_0 value (see eq 6) than other halide ion complexes. The β_0 value of $I^-@B_{10}H_{14}$ complex is about 3 times larger than 1076 a.u. of a prototypical NLO molecule of p-nitroaniline.[31] This implies that with a specific frequency of laser light, that is, off-resonant frequency with respect to 2.709/2 = 1.35 eV, the $I^-@B_{10}H_{14}$ type of compounds can be certainly expected for frequency doubling and other NLO applications. Because the $I^-@B_{10}H_{14}$ complex shows the largest β_0 value among other halide ion complexes, it has been further modified to get more polarization by the bottom positions in systems of sets B and C. The β_0 values of systems $\mathbf{B_1}$ and $\mathbf{B_2}$ are 3092 and 3696 a.u., which are 8 and 29% larger than $I^-@B_{10}H_{14}$ complex,

Table 1. Geometrical Parameters with Bond Distances (Å) and Bond Angles (θ) for $I^-@2,4\text{-}I_2B_{10}H_{12}$ Complex at the B3LYP/6-31G* Level of Theory

bond length (Å)	exptl[a] bond length (Å)	calcd bond length (Å)	bond angle (θ)	exptl bond angle (θ)	calcd bond angle (θ)
B_1–B_2	1.781	1.775 (1.771)[b]	B_2–B_1–B_3	60.1	59.81 (59.88)
B_2–B_6	1.744	1.734 (1.732)	B_2–B_1–B_5	58.9	60.74 (60.80)
B_2–B_5	1.753	1.787 (1.785)	B_3–B_1–B_4	60.4	59.81 (59.88)
B_2–I_2	2.181	2.221 (2.202)	B_3–B_1–B_{10}	108.6	107.37 (107.29)
B_3–B_7	1.746	1.760 (1.755)	I_2–B_2–B_1	121.0	120.42 (120.44)
B_7–B_8	1.949	1.953 (1.956)	B_2–B_6–B_7	61.9	60.99 (61.15)
B_6–I^-	3.526	3.624 (3.566)	B_1–B_2–B_5	60.6	59.19 (59.17)
B_6–B_7	1.794	1.787 (1.775)	B_1–B_2–B_7	105.4	106.60 (106.28)
B_6–μH_6		1.335 (1.336)	I_1–B_2–B_6	120.1	119.46 (119.96)

[a]Experimental values have been taken from ref 22. [b]Values in parentheses are at the CCSD/6-31G* level of theory.

dx.doi.org/10.1021/jp209385b | J. Phys. Chem. A 2012, 116, 1417–1424

Table 2. All Adopted Chemical Models with Their Atomic Distances (Å) between $B_{6/9}$ Atoms and Halide Ions X, Polarizabilities (α_0 in a.u.), First Hyperpolarizabilities (β_0 in a.u.),[a] and Their Main Individual Nonzero (β_{xxz}, β_{yyz}, and β_{zzz}) Components at the B3LYP/6-31G* Level of Theory

chemical models	system label	X−$B_{6/9}$	α_0	β_{xxz}	β_{yyz}	β_{zzz}	β_0
Set A							
$F^-@B_{10}H_{14}$	$\mathbf{A_1}$	2.712	140	20	28	533	367
$Cl^-@B_{10}H_{14}$	$\mathbf{A_2}$	3.302	159	10	29	1749	1088
$Br^-@B_{10}H_{14}$	$\mathbf{A_3}$	3.382	173	101	87	1563	1125
$I^-@B_{10}H_{14}$	$\mathbf{A_4}$	3.748	161	62	95	4504	2859
Set B							
$I^-@2,4\text{-}I_2B_{10}H_{12}$	$\mathbf{B_1}$	3.624	224	65	258	4616	3092
$I^-@1,3\text{-}I_2B_{10}H_{12}$	$\mathbf{B_2}$	3.661	230	86	136	5791	3696
$I^-@2,4\text{-}F_2B_{10}H_{12}$	$\mathbf{B_3}$	3.697	161	61	−3	4090	2512
Set C							
$I^-@2,4\text{-}Li_2B_{10}H_{12}$	$\mathbf{C_1}$	3.942	327	2565	17828	24058	34827
$I^-@2,4\text{-}Na_2B_{10}H_{12}$	$\mathbf{C_2}$	3.881	899	3571	15966	25339	34740
$I^-@2,4\text{-}K_2B_{10}H_{12}$	$\mathbf{C_3}$	3.946	1442	8429	29514	40822	62436
Set BS							
$[I^-@2,4\text{-}I_2B_{10}H_{12}]$ PCM	$\mathbf{B_1S}$	3.785	274	88	172	10479	6547
$[I^-@1,3\text{-}I_2B_{10}H_{12}]$ PCM	$\mathbf{B_2S}$	3.825	281	−214	188	11271	6737
$[I^-@2,4\text{-}F_2B_{10}H_{12}]$ PCM	$\mathbf{B_3S}$	3.856	193	105	−09	7511	4603
Set BNa							
$[I^-@2,4\text{-}I_2B_{10}H_{12}]Na$	$\mathbf{B_1Na}$	3.731	296	462	349	13380	8839
$[I^-@1,3\text{-}I_2B_{10}H_{12}]Na$	$\mathbf{B_2Na}$	3.782	299	28	570	14014	9006
$[I^-@2,4\text{-}F_2B_{10}H_{12}]Na$	$\mathbf{B_3Na}$	3.794	201	190	64	9509	5959

[a]Conversion factors for β_0 from a.u. to SI and esu units: 1 a.u. = 3.26361×10^{-53} C^3 m^2 J^{-2} = 8.639418×10^{-33} esu.

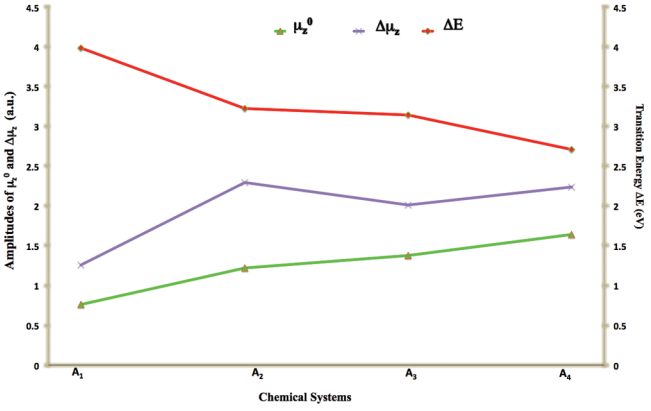

Figure 2. Graphical representation of the amplitudes of transition moments μ_z^0 (a.u.), change of dipole moments between the ground and crucial excited states $\Delta\mu_z$ (a.u.), and transition energies ΔE (eV) for halide ion complexes ($\mathbf{A_1}$, $\mathbf{A_2}$, $\mathbf{A_3}$, $\mathbf{A_4}$) of $B_{10}H_{14}$ listed in Table 3.

respectively. Furthermore, the individual tensor element β_{zzz} is shown to be much larger than other β_{ijk} tensors, the feature of which gives advantage to these systems to be measured easily by a hyper-Rayleigh scattering. The fluoro substitution at 2,4 positions of $I^-@B_{10}H_{14}$ complex has been also checked in system $\mathbf{B_3}$ and it reduces the β_0 by 12%, which might be due to its shorter bond length and π-back interaction of fluorine with borane cage.[32] A more prominent and robust increase of β_0 value has been observed in systems of set C with alkali metals substitutions at 2,4 positions of $I^-@B_{10}H_{14}$ complex. The β_0 values of 34827, 34740, and 62436 a.u. have been calculated for systems $\mathbf{C_1}$, $\mathbf{C_2}$ and $\mathbf{C_3}$, respectively (see Table 2). The systems in set C show lower transition energies along with larger transition moment amplitudes associated with the increase of electron donating property. These transition energies, which are significantly reduced than that of their parent $I^-@B_{10}H_{14}$ complex ($\mathbf{A_4}$), vary in the order $\mathbf{C_1} \sim \mathbf{C_2} > \mathbf{C_3}$, while the transition moment amplitudes do in the order $\mathbf{C_1} < \mathbf{C_2} \sim \mathbf{C_3}$. These variations are understood by the extent of the diffused s-type character of alkali atoms (Li < Na < K) involved in the molecular orbitals HOMO and LUMO+1 (see Figure 4) of the

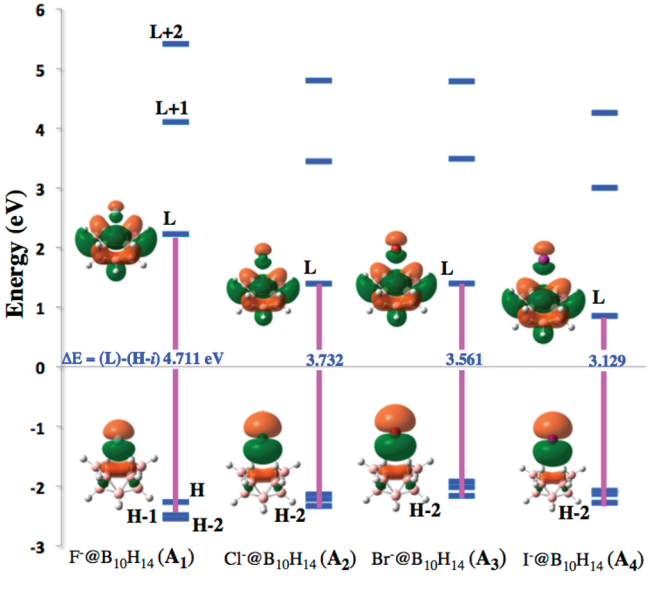

Figure 3. Schematic representation of molecular orbitals [HOMO(H)-*i*, LUMO(L)+*j*] and the energy gaps (eV) between orbitals involved in transitions for chemical systems of set A.

substituted complexes and consequently provide an increase in the order of $|\beta_{zzz}|$ values: $\mathbf{C_1} < \mathbf{C_2} < \mathbf{C_3}$ (see eq 6). From Table 2, it can be seen that the β_0 value of system $\mathbf{C_3}$ is about 22 times

dx.doi.org/10.1021/jp209385b | J. Phys. Chem. A 2012, 116, 1417−1424

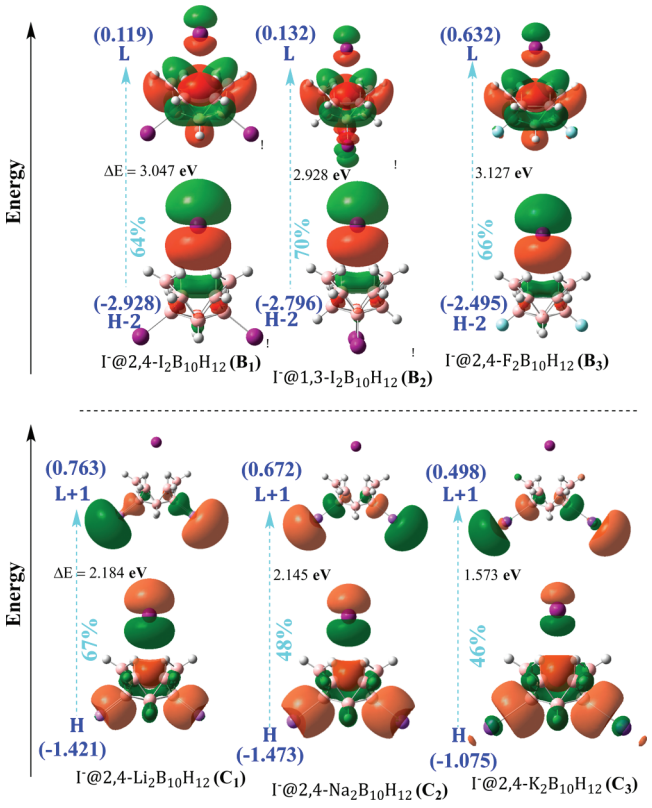

Figure 4. Frontier molecular orbitals with their orbital energies (values in parentheses, eV), orbital energy gaps [ΔE = LUMO(L)+j − HOMO(H)-i] and percentage contributions for crucial transitions of systems in sets B and C.

larger than its parent $I^-@B_{10}H_{14}$ complex ($\mathbf{A_4}$). Interestingly, the β_0 value of system $\mathbf{C_3}$ is also 2 and 9 times larger than our previously designed $Li@B_{10}H_{14}$[21] and Li et al.'s Li@calix[4]-pyrrole,[33] respectively. The above results represent that the substitutions of iodine and alkali metal atoms at the bottom of $I^-@B_{10}H_{14}$ complex has marked effects on its β_0 value. The present substitution effect is thus expected to be useful for getting a totally inorganic material with robustly large NLO response.

Because systems $\mathbf{B_1}$ and $\mathbf{B_2}$ of set B are reported in an experimental study, we have chosen the systems of set B to check the effect of solvent and counter positive ions on their polarizations. The electro-optical properties of systems in sets BS and BNa are obtained by the PCM method and with counterion of Na, respectively. A careful analysis of these results shows that solvent has increasing tendency not only on polarizability but also on the first hyperpolarizability (see Table 2). The β_0 values of systems in set BS are larger and become almost double to the values of their respective systems in set B, that is, without solvent effect. The validity of this result should be confirmed by using more precise and realistic models like QM/MM method because the PCM method with the FF approach is reported to somewhat overshoot the polarizability of a molecule in solution.[34] A similar but more pronounced effect has been seen in systems of set BNa where the β_0 values become almost 3 times to their respective systems without counterion and solvent effects. Because the stable position of Na ion has been found near the bottom of the $I^-@2,4\text{-}I_2B_{10}H_{12}$ complex along its C_2 axis, it has significantly increased the dipole moment differences $\Delta\mu_z$ similar to the solvent effects in set BS. Besides this, the lower transition energies and higher transition moments of the systems in set BNa lead to their larger β_0 amplitudes as compared to those with solvent effects in set BS.

3.3. Origin of First Hyperpolarizability. In several previous reports,[21,33,35−38] the origin of β_0 values has always been traced from only the transition energies. In the present study, however, to perform a more complete analysis of a full set of parameter dependences of β, we have performed the TD-DFT calculations to obtain the crucial excited states of all adopted chemical systems. From Table 3, it can be seen that

Table 3. TD-DFT Results for All Adopted Chemical Models Including Their Transition Moments $|\mu_z^0|$, Transition Energies ΔE, Change of Dipole Moments between the Ground and Crucial Excited States $\Delta\mu_z = \mu_{ee} - \mu_{gg}$ and β_{zzz} Value (a.u.) According to the Two-Level Expression (T-Convention) $\beta_{zzz} = 2 \times \{3\Delta\mu_z(\mu_z^0/\Delta E)^2\}$

systems	electronic excitation	ΔE /eV	$\lvert\mu_z^0\rvert$/ a.u.	$\Delta\mu_z$/ a.u.	major contribution	β_{zzz}/ a.u.
			Set A			
$\mathbf{A_1}$	$S_0 \rightarrow S_2$	4.111	0.579	1.256	H-1 → L	202
$\mathbf{A_2}$	$S_0 \rightarrow S_3$	3.291	1.144	2.294	H-2 → L	1460
$\mathbf{A_3}$	$S_0 \rightarrow S_3$	3.189	1.278	2.012	H-2 → L	1718
$\mathbf{A_4}$	$S_0 \rightarrow S_3$	2.709	1.640	2.235	H-2 → L	4064
			Set B			
$\mathbf{B_1}$	$S_0 \rightarrow S_3$	2.694	1.769	2.265	H-2 → L	4338
$\mathbf{B_2}$	$S_0 \rightarrow S_3$	2.588	1.972	2.453	H-2 → L	6332
$\mathbf{B_3}$	$S_0 \rightarrow S_3$	2.743	1.713	2.487	H-2 → L	4308
			Set C			
$\mathbf{C_1}$	$S_0 \rightarrow S_2$	1.736	2.152	4.768	H → L+1	32552
$\mathbf{C_2}$	$S_0 \rightarrow S_3$	1.853	3.014	3.000	H → L+1	35936
$\mathbf{C_3}$	$S_0 \rightarrow S_3$	1.415	3.152	2.449	H → L+1	53988
			Set BS			
$\mathbf{B_1S}$	$S_0 \rightarrow S_3$	2.856	1.674	5.025	H-2 → L	7668
$\mathbf{B_2S}$	$S_0 \rightarrow S_3$	2.795	1.819	5.562	H-2 → L	10462
$\mathbf{B_3S}$	$S_0 \rightarrow S_3$	3.000	1.538	5.273	H-2 → L	6146
			Set BNa			
$\mathbf{B_1Na}$	$S_0 \rightarrow S_3$	2.758	1.861	4.200	H-2 → L	9300
$\mathbf{B_2Na}$	$S_0 \rightarrow S_3$	2.738	1.884	6.872	H-2 → L	14446
$\mathbf{B_3Na}$	$S_0 \rightarrow S_3$	2.880	1.646	6.596	H-2 → L	9576

the transition energy is far from sufficient to explain the difference of first hyperpolarizabilities among chemical systems in all the sets, so we employ a two-level expression given by[39]

$$\beta_0 \cong \beta_{zzz} = 3\Delta\mu_z\left(\frac{\mu_z^0}{\Delta E}\right)^2 \quad (6)$$

where ΔE is the transition energy, μ_z^0 is the transition moment, and $\Delta\mu_z$ is the dipole moment difference between the ground and crucial excited states along the z-axis. The excited-state dipole moments were calculated by using the FF method, which involves the evaluation of the changes in excitation energies in the presence of external electric fields of ±0.001 a.u.[40] The β_{zzz} values have been converted into so-called T-convention (Taylor series) simply by factors of 2!, which is defined in the following expression given by Willetts et al.[41]

$$\beta^T = 2\beta^B \quad (7)$$

Based on eq 7, we have multiplied the β_{zzz} values calculated by a two-level approximation with 2 to convert these into T-

dx.doi.org/10.1021/jp209385b | J. Phys. Chem. A 2012, 116, 1417−1424

convention values. Finally, we have drawn the graph between β_{zzz} calculated by the FF method (T-convention, eq 1) and by the two-state approximation (T-convention, eq 7), as shown in Figure 6.

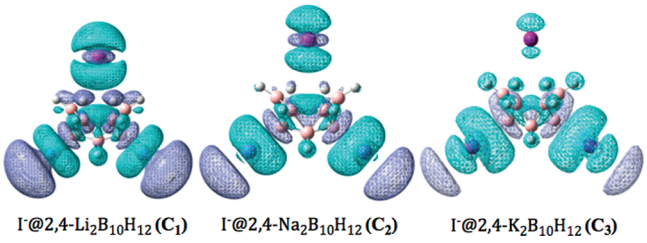

Figure 5. Electron density difference maps (EDD) of systems in set C between their ground state and excited state of interest with isovalue (0.02 a.u.). The cyan-blue color denotes a loss and the violet color a gain of electron density.

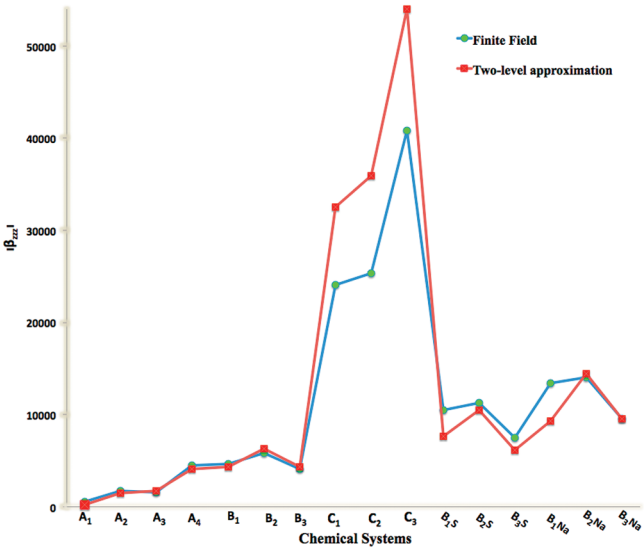

Figure 6. Comparison of the amplitudes of β_{zzz} values (a.u.) calculated by the FF method and two-level approximation for different adopted chemical systems.

From the graph in Figure 6, the following points can be concluded: (i) A good semiquantitative agreement has been found between two independently calculated β_{zzz} values, that is, with the FF method and two-level approximation where the latter is often used by the experimentalists to design new NLO materials. (ii) Similar to some previous reports,[42] the β_{zzz} values obtained by the two-level method are slightly large as compared to those by the FF method especially in set C, which might be due to their lowest energy transitions serving as a the decisive factors for β_{zzz} values of set C. (iii) The systems in set BS has higher β_{zzz} values by the FF method in combination with PCM model, which is in accordance to our previous studies where the FF method combined with PCM model overshoots gas phase β_{zzz} values.[34] (iv) It can be further noted that only transition energies are not the decisive factors for all adopted systems. For example in sets BS and BNa, the $\Delta\mu_z$ values also play an important role to enhance the $|\beta_{zzz}|$ values.

3.4. Frontier Molecular Orbital Analysis. Because TD-DFT results are concerned with the orbital transition properties, we have presented the frontier molecular orbitals (FMOs) along with their relative energies involved in the crucial transitions for systems in sets A, B, and C (see Figures 3 and 4). For systems in set A, their crucial transitions involve HOMO-2 to LUMO, except in system $\mathbf{A_1}$, which involves HOMO-1 to LUMO. From the FMOs analysis, an effective orbital interaction between halide ions and $B_{10}H_{14}$ basket can also be observed. The occupied orbitals show that the p-orbital of halide ions are directed toward the electron deficient open face of decaborane basket, resulting in effective orbital interactions in $X^-@B_{10}H_{14}$ complexes and its derivatives (see Figure 3). In all the systems of sets A and B, the crucial transition involves a significant charge transfer from p-orbital of halide ion to the electron deficient decaborane basket. The extent of this charge transfer is different in different halide ion decaborane complexes and in their derivatives. For example, the HOMO-2−LUMO energy gap of the $I^-@B_{10}H_{14}$ complex is lower than those of other $X^-@B_{10}H_{14}$ (X = F, Cl, and Br) complexes, the feature of which causes a lower energy transition with higher transition moment amplitude. More specifically, the higher transition moment amplitude is associated with larger transition density amplitude between these MOs, where both the overlap between these MOs and the charge transfer length become larger. The FMOs of systems in set B are also similar to their parent $I^-@B_{10}H_{14}$ complex but have smaller orbital energy gaps in set B, probably due to the bottom substituents. For example, system $\mathbf{B_2}$ has the lowest energy gap and it has some orbital distributions on I_1 and I_3 atoms in the bottom of LUMO of B2 (Figure 4), which stabilizes LUMO of B_2 as compared to its parent and other systems in set B.

For systems in set C, their crucial transitions involve HOMO to LUMO+1 orbitals. A further increase of charge transfer can be observed in FMOs of 2,4-alkali metal-substituted complexes, which involves a slightly long-rang charge transfer from HOMO (localized on iodine ion and borane basket) to its Rydberg-type LUMO+1 (localized on 2,4-alkali metal atoms) with lower transition energies (see Figure 4). As the diffused s-orbitals are on alkali metal atoms and the extent of their diffused character increases from Li < Na < K due to involvement of their 2s, 3s, and 4s orbitals to form LUMO+1 of these complexes, respectively, which ultimately cause the lowering of transition energy in their crucial transitions. The increase in the transition moment, which is understood by transition density as going from Li to K, can be explained primarily by the variation in the transition density in boron basket region, where the transition density is extended to alkali metal (this tendency is increased as Li < Na < K), due to the disappearance of distribution of I^- in the LUMO+1. Unlike the transition energies and transition moments, the changes in the dipole moment differences for Li-, Na-, and K-substituted complexes are not favorable in increasing the β_0 values. The decrease of amplitude of dipole moment difference (Li > Na > K) can be explained by electron density difference (EDD) maps for systems in set C (as shown in Figure 5), which can intuitively demonstrate the electron movement due to either the polarization or charge transfer effect between the iodide ion and electron deficient borane fragments. The primary charge changes in the z direction (decrease in I and increase in alkali-metal regions), which increases in $\Delta\mu_z$ and is predicted to be larger for Li case than for Na and K cases due to the larger population in I and alkali-metal regions in the Li case than in Na and K cases, as seen from Figure 5. As going from Li to K through Na, the distribution on I in HOMO decreases due to the larger diffused character of K > Na > Li, which is also found to determine the extension of alkali atom distributions of L+1

dx.doi.org/10.1021/jp209385b | J. Phys. Chem. A 2012, 116, 1417−1424

(see Figure 4). Because the positive dipole moment differences are caused by the CT from I to boron basket and alkali atoms, the difference in amplitudes are found to decrease as going from Li to K and are calculated to be 4.768, 3.00, and 2.449 a.u. Nevertheless, with two level expressions, the marked variation of transition moment differences and transition energies overcome the slight effects of dipole moment differences. Hence, these charge transfer transitions are the key factors to increase NLO response sharply in alkali metal derivatives of $I^-@B_{10}H_{14}$ complexes.

4. CONCLUSIONS

A comparative DFT study on different halo complexes of $B_{10}H_{14}$ and its derivatives has been performed. The results show that their polarizabilities and first hyperpolarizabilities are partly associated with noncovalent charge-transfer interactions between halide ions and $B_{10}H_{14}$ complexants. The following conclusions can be obtained in the theoretical framework of the present DFT calculations:

(1) The polarizability and first hyperpolarizability values increase in different decaborane halide ion complexes $X^-@B_{10}H_{14}$ (X = F, Cl, Br, and I) as moving down the group from F to I that is due to the decrease of electron affinity and increase in anionic size from F to I.

(2) The two experimentally reported complexes $I^-@B_{10}H_{14}$ and $I^-@2,4\text{-}I_2B_{10}H_{12}$ are found to possess considerably large β_0 values of 2859 and 3092 a.u., respectively. These values show further increments and become 2 and 3 times larger by considering the solvent and counterion effects, respectively.

(3) Interestingly, the 2,4-alkali metal-substituted $I^-@B_{10}H_{14}$ complexes showed remarkably large NLO response with β_0 values as large as 62436 a.u. for $I^-@2,4\text{-}K_2B_{10}H_{12}$ complex, which have been explained in terms of their transition energies, FMOs and EDD plots.

(4) The TD-DFT results were implemented in two-level approximation to obtain the insights for the origin of first hyperpolarizability in different adopted chemical systems. The transition energies play decisive role in large β_0 values of alkali metal substituted compounds but change of dipole moments between ground and crucial excited states also become important by considering the solvent and counterion effects.

(5) Thus, our present investigation reveals that $I^-@B_{10}H_{14}$ complex not only exhibits significantly large amplitudes of first hyperpolarizabilities, but also can be finely tuned to get a robust NLO response.

■ ASSOCIATED CONTENT

Supporting Information

The results of a comparison of the first hyperpolarizability values with different extended basis sets on $I^-@2,4\text{-}I_2\text{–}B_{10}H_{12}$ complex in Table S1. Similar assessment results of polarizability and first hyperpolarizability values calculated by different methods using the CCSD optimized geometry of $I^-@2,4\text{-}I_2\text{–}B_{10}H_{12}$ complex (Table S2). This material is available free of charge via the Internet at http://pubs.acs.org.

■ AUTHOR INFORMATION

Corresponding Author

*Fax: +81-6-6850-6268. E-mail: mnaka@cheng.es.osaka-u.ac.jp.

■ ACKNOWLEDGMENTS

This work is supported by a Grant-in-Aid for Scientific Research (No. 21350011) from Japan Society for the Promotion of Science (JSPS) and the global COE (center of excellence) program "Global Education and Research Center for Bio-Environmental Chemistry" of Osaka University. S.M. acknowledges the funding (No. P11335) for a post-doctorate fellowship by JSPS. S.M. also acknowledges the guidelines and help of Mrs. Iffat Shabbiri for the completion of this article.

■ REFERENCES

(1) Franken, P.; Hill, A.; Peters, C.; Weinreich, G. *Phys. Rev. Lett.* **1961**, *7*, 118.

(2) (a) Aubert, V.; Ordronneau, L.; Escadeillas, M.; Williams, J. A. G.; Boucekkine, A.; Coulaud, E.; Dragonetti, C.; Righetto, S.; Roberto, D.; Ugo, R.; Valore, A.; Singh, A.; Zyss, J.; Ledoux-Rak, I.; Le Bozec, H.; Guerchais, V. *Inorg. Chem.* **2011**, *50*, 5027–5038. (b) Choi, E.-Y.; Kim, P.-J.; Jazbinsek, M.; Kim, J.-T.; Lee, Y. S.; Guanter, P.; Lee, S. W.; Kwon, O. P. *Cryst. Growth Des.* **2011**, DOI: 10.1021/cg200320f. (c) Hrobarik, P.; Sigmundova, I.; Zahradnik, P.; Kasak, P.; Arion, V.; Franz, E.; Clays, K. *J. Phys. Chem. C* **2010**, *114*, 22289–22302. (d) Badaeva, E.; Harpham, M. R.; Guda, R.; Suzer, O.; Ma, C.-Q.; Bauerle, P.; Goodson, T.; Tretiak, S. *J. Phys. Chem. B* **2010**, *114*, 15808–15817. (e) Oliva, M. M.; Casado, J.; Navarrete, J. T. L.; Patchkovskii, S.; Goodson, T.; Harpham, M. R.; Seixas de Melo, J. S.; Amir, E.; Rozen, S. *J. Am. Chem. Soc.* **2010**, *132*, 6231–6242. (f) Clark, T. B.; Orr, M. E.; Flynn, D. C.; Goodson, T. *J. Phys. Chem. C* **2011**, *115*, 7331–7338.

(3) (a) Burland, D. M., Ed. Optical Nonlinearities in Chemistry. In *Chem. Rev.*; American Chemical Society: Washington, DC, 1994, Vol. *94*. (b) Zyss, J., Ed. Molecular Nonlinear Optics: Materials. In *Physics and Devices*; Academic Press: New York, 1994. (c) Champagne, B.; Kirtman, B. In *Handbook of Advanced Electronic and Photonic Materials and Devices*; Nalwa, H.S., Ed.; Academic Press: New York, 2001; Vol *9*, Chap. 2, p 63.

(4) (a) Coe, B. J.; Harris, J. A.; Brunschwig, B. S. *J. Phys. Chem. A* **2002**, *106*, 897–905. (b) Clays, K.; Coe, B. *J. Chem. Mater.* **2003**, *15*, 642–648. (c) Coe, B. J.; Harris, J. A.; Brunschwig, B. S.; Garin, J.; Orduna, J.; Coles, S. J.; Hursthouse, M. B. *J. Am. Chem. Soc.* **2004**, *126*, 10418–10427. (d) Coe, B. J.; Harris, J. A.; Brunschwig, B. S.; Asselberghs, I.; Clays, K.; Garin, J.; Orduna, J. *J. Am. Chem. Soc.* **2005**, *127*, 13399–13410. (e) Coe, B. J.; Harris, J. A.; Jones, L. A.; Brunschwig, B. S.; Song, K.; Clays, K.; Garin, J.; Orduna, J.; Coles, S. J.; Hursthouse, M. B. *J. Am. Chem. Soc.* **2005**, *127*, 4845–4859.

(5) (a) Cecchet, F.; Lis, D.; Guthmuller, J.; Champagne, B.; Fonder, G.; Mekhalif, Z.; Caudano, Y.; Mani, A. A.; Thiry, P. A.; Peremans, A. *J. Phys. Chem. C* **2010**, *114*, 4106–4113. (b) Sanguinet, L.; Pozzo, J. L.; Rodriguez, V.; Adamietz, F.; Castet, F.; Ducasse, L.; Champagne, B. *J. Phys. Chem. B* **2005**, *109*, 11139. (c) Plaquet, A.; Guillaume, M.; Champagne, B.; Rougier, L.; Mancois, F.; Rodriguez, V.; Pozzo, J. L.; Ducasse, L.; Castet, F. *J. Phys. Chem. C* **2008**, *112*, 5638. (d) Mancois, F.; Pozzo, J. L.; Adamietz, F.; Rodriguez, V.; Ducasse, L.; Castet, F.; Plaquet, A.; Champagne, B. *Chem.—Eur. J.* **2009**, *15*, 2560. (e) Bogdan, E.; Plaquet, A.; Antonov, L.; Rodriguez, V.; Ducasse, L.; Champagne, B.; Castet, F. *J. Phys. Chem. C* **2010**, *114*, 12760–12768.

(6) Pati, S. K.; Marks, T. J.; Ratner, M. A. *J. Am. Chem. Soc.* **2001**, *123*, 7287.

(7) Facchetti, A.; Hutchison, G. R.; Keinan, S.; Ratner, M. A. *Inorg. Chim. Acta., Int. Ed.* **2005**, *44*, 7922.

(8) Isborn, C. M.; Davidson, E. R.; Robinson, B. H. *J. Phys. Chem. A* **2006**, *110*, 7189.

(9) Nakano, M.; Ohta, S.; Tokushima, K.; Kishi, R.; Kubo, T.; Kamada, K.; Ohta, K.; Champagne, B.; Botek, E.; Takahashi, H. *Chem. Phys. Lett.* **2007**, *443*, 95–101.

(10) Zhang, J. H.; Hu, C. L.; Xu, X.; Kong, F.; Mao, J. G. *Inorg. Chem.* **2011**, *50*, 1973–1982.

(11) Aubert, V.; Ordronneau, L.; Escadeillas, M.; Williams, J. A. G.; Boucekkine, A.; Coulaud, E.; Dragonetti, C.; Righetto, S.; Roberto, D.; Ugo, R.; Valore, A.; Singh, A.; Zyss, J.; Rak, I. L.; Bozec, H. L.; Guerchais, V. *Inorg. Chem.* **2011**, *50*, 5027−5038.
(12) (a) Burland, D. M. *Chem. Rev.* **1994**, *94*, 1. (b) Zyss, J.; Ledoux, I. *Chem. Rev.* **1994**, *94*, 77−105. (c) Berkovic, G.; Krongauz, V.; Weiss, V. *Chem. Rev.* **2000**, *100*, 1741−1754. (d) Delaire, J. A.; Nakatani, K. *Chem. Rev.* **2000**, *100*, 1817−1846. (e) Coe, B. J. *Acc. Chem. Res.* **2006**, *39*, 383. (f) Radhakrishnan, T. P. *Acc. Chem. Res.* **2008**, *41*, 367. (g) Ray, P. C. *Chem. Rev.* **2010**, *110*, 5332−5365.
(13) Chen, C. T.; Wu, Y. C.; Jiang, A. D.; Wu, B. C.; You, G. M.; Li, R. K.; Lin, S. J. *J. Opt. Soc. Am. B* **1989**, *6*, 616−621.
(14) Chen, C. T.; Wu, B. C.; Jiang, A. D.; You, G. M. *Sci. Sin., Ser. B* **1985**, *28*, 235−243.
(15) Li, R. K.; Chen, P. *Inorg. Chem.* **2010**, *49*, 1561−1565.
(16) Chen, C. T.; Wu, Y. C.; Li, R. K. *J. Cryst. Growth* **1990**, *99*, 790−798.
(17) Munoz, B. M.; Santillan, R.; Rodriguez, M.; Mendez, J. M.; Romero, M.; Farfan, N.; Lacroix, P. G.; Nakatani, K.; Ortiz, G. R.; Maldonado, J. L. *J. Organomet. Chem.* **2008**, *693*, 1321−1334.
(18) Muhammad, S.; Xu, H. L.; Liao, Y.; Kan, Y. H.; Su, Z. M. *J. Am. Chem. Soc.* **2009**, *131*, 11833.
(19) Muhammad, S.; Xu, H. L.; Su, Z. M. *J. Phys. Chem. A* **2011**, *115*, 923−931.
(20) Li, Y.; Sneddon, L. G. *J. Am. Chem. Soc.* **2008**, *130*, 11494−11502.
(21) Del Bene, J. E.; Elguero, J.; Alkorta, I.; Yaneez, M.; Mo, O. *J. Phys. Chem. A* **2007**, *111*, 419−421.
(22) Wermer, J. R.; Hollander, O.; Huffman, J. C.; Bauer, J. A. K.; Dou, D.; Hsu, L. Y.; Leussing, D. L.; Shore, S. G. *Inorg. Chem.* **1995**, *34*, 3065.
(23) (a) Koch, W.; Holthausen, M. C. *A Chemist's Guide to Density Functional Theory*; Wiley-VCH: Weinheim, Germany, 2000. (b) Adamo, C.; di Matteo, B. V. *Adv. Quantum Chem.* **1999**, *36*, 4.
(24) (a) Hay, P. J.; Wadt, W. R. *J. Chem. Phys.* **1985**, *82*, 270. (b) Hay, P. J.; Wadt, W. R. *J. Chem. Phys.* **1985**, *82*, 284. (c) Hay, P. J.; Wadt, W. R. *J. Chem. Phys.* **1985**, *82*, 299.
(25) Pople, J. A.; Head-Gordon, M.; Raghavachari, K. *J. Chem. Phys.* **1987**, *87*, 5968−75.
(26) Casida, M. K.; Jamorski, C.; Casida, K. C.; Salahub, D. R. *J. Chem. Phys.* **1998**, *108*, 4439−4449.
(27) Cossi, M.; Rega, N.; Scalmani, G.; Barone, V. *J. Comput. Chem.* **2003**, *24*, 669−681.
(28) Frisch, M. J.; Trucks, G. W.; Schlegel, H. B.; Scuseria, G. E.; Robb, M. A.; Cheeseman, J. R.; Montgomery, J. A., Jr.; Vreven, T.; Kudin, K. N.; Burant, J. C.; Millam, J. M.; Iyengar, S. S.; Tomasi, J.; Barone, V.; Mennucci, B.; Cossi, M.; Scalmani, G.; Rega, N.; Petersson, G. A.; Nakatsuji, H.; Hada, M.; Ehara, M.; Toyota, K.; Fukuda, R.; Hasegawa, J.; Ishida, M.; Nakajima, T.; Honda, Y.; Kitao, O.; Nakai, H.; Klene, M.; Li, X.; Knox, J. E.; Hratchian, H. P.; Cross, J. B.; Bakken, V.; Adamo, C.; Jaramillo, J.; Gomperts, R.; Stratmann, R. E.; Yazyev, O.; Austin, A. J.; Cammi, R.; Pomelli, C.; Ochterski, J. W.; Ayala, P. Y.; Morokuma, K.; Voth, G. A.; Salvador, P.; Dannenberg, J. J.; Zakrzewski, V. G.; Dapprich, S.; Daniels, A. D.; Strain, M. C.; Farkas, O.; Malick, D. K.; Rabuck, A. D.; Raghavachari, K.; Foresman, J. B.; Ortiz, J. V.; Cui, Q.; Baboul, A. G.; Clifford, S.; Cioslowski, J.; Stefanov, B. B.; Liu, G.; Liashenko, A.; Piskorz, P.; Komaromi, I.; Martin, R. L.; Fox, D. J.; Keith, T.; Al-Laham, M. A.; Peng, C. Y.; Nanayakkara, A.; Challacombe, M.; Gill, P. M. W.; Johnson, B.; Chen, W.; Wong, M. W.; Gonzalez, C.; Pople, J. A. *Gaussian 09*, Revision B.01; Gaussian, Inc.: Wallingford, CT, 2009.
(29) Gaines, D. F. *Inorg. Chem.* **2000**, *39*, 1812−1813.
(30) (a) Bondi, A. *J. Phys. Chem.* **1964**, *68*, 441−452. (b) Rowland, R. S; Taylor, R. *J. Phys. Chem.* **1996**, *100*, 7384−7391.
(31) Soscun, H.; Castellano, O.; Bermudez, Y.; Toro, C.; Cubillan, N.; Hinchliffe, A.; Phu, X. N. *Int. J. Quantum Chem.* **2006**, *106*, 1130−1137.
(32) Ewing, W. C.; Carroll, P. J.; Sneddon, L. G. *Inorg. Chem.* **2008**, *47*, 8580.
(33) Chen, W.; Li, Z. R.; Wu, D.; Li, Y.; Sun, C. C.; Gu, F. L. *J. Am. Chem. Soc.* **2005**, *127*, 10977−10981.
(34) Takahashi, H.; Kitaura, M.; Kishi, R.; Ohta, S.; Okaji, R.; Furukawa, S.; Nakano, M. *Comput. Lett.* **2007**, *3*, 441−448.
(35) Jing, Y. Q.; Li, Z. R.; Wu, D.; Li, Y.; Wang, B. Q. *J. Phys. Chem. B* **2006**, *110*, 11725−11729.
(36) Xu, H. L.; Li, Z. R.; Wu, D.; Ma, F.; Li, Z. J. *J. Phys. Chem. C* **2009**, *113*, 4984−4986.
(37) Chen, W.; Li, Z. R.; Wu, D; Li, Y.; Sun, C. C. *J. Phys. Chem. A* **2005**, *109*, 2920−2924.
(38) Chen, W.; Li, Z. R.; Wu, D.; Li, Y.; Sun, C. C.; Gu, F. L.; Aoki, Y. *J. Am. Chem. Soc.* **2006**, *128*, 1072−1073.
(39) (a) Oudar, J. L.; Chemla, D. S. *J. Chem. Phys.* **1977**, *66*, 2664−2668. (b) Oudar, J. L. *J. Chem. Phys.* **1977**, *67*, 446−457.
(40) Coe, B. J.; Harries, J. L.; Helliwell, M.; Jones, L. A.; Asselberghs, I.; Clays, K.; Burnschwig, B. S.; Harris, J. A.; Garin, J.; Orduna, J. *J. Am. Chem. Soc.* **2006**, *128*, 12192−12204.
(41) Willetts, A.; Rice, J. E.; Burland, D. M.; Shelton, D. P. *J. Chem. Phys.* **1992**, *97*, 7590.
(42) Champagne, B.; Kirtman, B. *J. Chem. Phys.* **2006**, *125*, 024101−7.